

## Band Structure and Infrared Absorption of Graphite

W. S. BOYLE AND P. NOZIÈRES\*  
*Bell Telephone Laboratories, Murray Hill, New Jersey*  
 (Received April 1, 1958)

The infrared optical properties of graphite single crystals have been calculated from a model of the band structure developed by group theory. These calculations have been compared with measurements of the emissivity and reflection coefficient of single crystals. At short wavelengths interband effects predominate; from the experimental results the maximum splitting of the  $\pi$  bands at a corner of the zone has been set at 0.56 electron volt. At longer wavelengths the intraband contributions become large, giving rise to plasma effects in the neighborhood of 25 microns. This gives an approximate value of the band overlap lying between 0.04 and 0.01 electron volt.

### INTRODUCTION

RECENTLY there have been several papers on the band structure of graphite. The approach has been to rely on group theory and perturbation methods to give the general topology of the bands and then to resort to experiment to obtain certain adjustable parameters which when determined give the exact band structure near the Fermi surface. McClure<sup>1</sup> and Nozières<sup>2</sup> have used the model developed by Slonczewski and Weiss<sup>3</sup> to discuss de Haas-Van Alphen and cyclotron resonance experiments. From their work the number of adjustable parameters has been reduced to two. This paper deals with the infrared properties of graphite and from experiment attempts to fix one of these remaining parameters.

In this paper we rely heavily on the validity of the model presented in the above papers and rather than try to measure the optical constants of graphite we have measured only one quantity, the power reflection coefficient at normal incidence. We make use of the theory to fit our experimentally observed curve over a large region of the spectrum and find that from these data, the short-wavelength region gives a value for the maximum band splitting of the  $\pi$  bands at the edge of the zone whereas at long wavelengths plasma effects predominate and give a measure of the total number of free carriers.

### EXPERIMENT

In order to obtain reliable optical data which can be related to the intrinsic properties of bulk graphite, we have performed our measurements on cleaved surfaces of single crystals of graphite. This sets rather severe restrictions on both the size and the optical quality of samples available. These considerations immediately preclude any of the usual optical techniques for measuring the optical constants  $n$  and  $k$  directly. The

quantity which we do measure, the reflection coefficient at normal incidence, has been obtained by two independent experiments.

In one case (the near infrared) we have determined the emissivity of a single crystal of graphite at 250°C, which is directly related to the reflection coefficient by Kirchoff's law. The experiment circumvents the necessity of obtaining a specularly reflecting surface and is also a sensitive way of measuring changes in the reflection coefficient when it is very close to unity.

In the second experiment we have measured directly the reflection coefficient at liquid helium temperatures. Here we have used a multiple reflection technique in order to obtain sufficient sensitivity and have also used a geometry such as to minimize the loss of light by nonspecular reflections. Of the two experiments, the first is by far the more reliable but because of the small power emitted cannot be used at wavelengths larger than 12 microns. The low-temperature measurements extend to 30 microns and pass through what we believe to be the plasma frequency. We shall now proceed to give a few of the relevant experimental details and the results obtained from each experiment.

To measure the emissivity, a single crystal of graphite was mounted on a brass backing plate and placed in a silver chloride tube. Dry nitrogen gas which had been heated was forced through the silver chloride tube and raised the temperature of the graphite to the desired value. The temperature was measured by a thermocouple which was attached directly to the brass backing plate. The graphite was imaged directly onto the entrance slit of an infrared spectrometer equipped with a rock salt prism. Radiation from the graphite was chopped and detected by a thermocouple. The complete spectrometer assembly was flushed with dry nitrogen to remove atmospheric absorption.

No attempt was made to obtain an absolute value for the emissivity, so the curve presented in Fig. 1 for the emissivity from 2 to 12 microns is in purely arbitrary units. Three corrections were applied to the data before obtaining the relative emissivity: (1) the emission and transmission coefficient of the silver chloride oven; (2) allowance for the fact that the signal obtained from the graphite was not the total radiative

\* Now at Laboratoire de Physique de l'École Normale Supérieure, 24 rue Lhomond, Paris V, France.

<sup>1</sup> J. W. McClure, *Proceedings of the Third Carbon Conference, Buffalo, New York, 1957* (to be published).

<sup>2</sup> P. Nozières, *Phys. Rev.* **109**, 1510 (1958).

<sup>3</sup> J. C. Slonczewski and P. R. Weiss, *Phys. Rev.* **99**, 636 (A) (1955). J. C. Slonczewski, Ph.D. thesis, Rutgers University, 1955 (unpublished).

transfer, but just the difference between the radiation from the graphite to the thermocouple and the thermocouple to the graphite; and (3) the transmission coefficient for the rocksalt prism. When we apply the corrections and normalize with respect to the black-body distribution, we obtain the curve shown in Fig. 1.

In the low-temperature experiments a sheet of graphite was mounted parallel to an aluminum mirror and 3 mm in front of it. Radiation was introduced at one end of this assembly and detected after about four reflections by a bolometer mounted directly at the exit. The sample and detector were both kept at liquid helium temperatures. Monochromatic radiation was obtained from an infrared spectrometer with suitable prisms to cover the range from 5 to 30 microns. The relative reflection coefficient of graphite was obtained by a twofold normalization process. First the signal level from the bolometer was determined as a function of wavelength with the graphite in place, and then this was compared to the signal obtained on a standard external thermocouple. This whole procedure was then repeated with an aluminum mirror in place of the graphite.

From these data and with the assumption that the reflection coefficient of aluminum is constant over this region, we obtain the relative reflectivity curve shown in Fig. 2.

### THEORY

We wish to apply the model of the graphite energy bands developed by Slonczewski and Weiss<sup>3</sup> to calculate the infrared properties of graphite single crystals. The model has been described by one of us<sup>2</sup> in relation to cyclotron resonance, and in this paper we shall use the

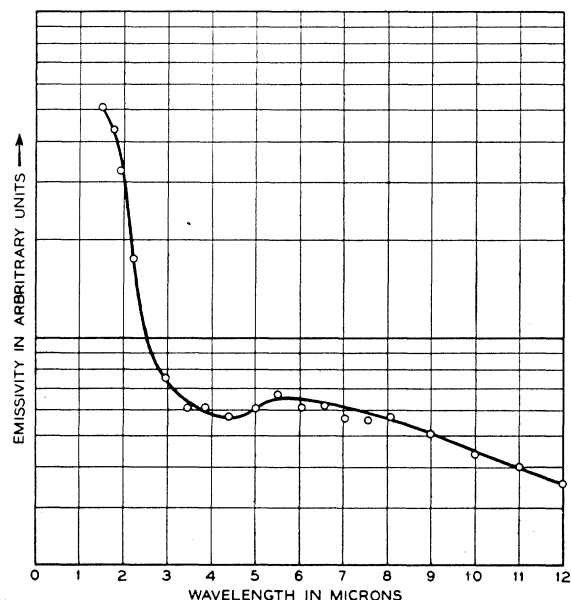


FIG. 1. The emissivity of a single crystal of graphite in arbitrary units.

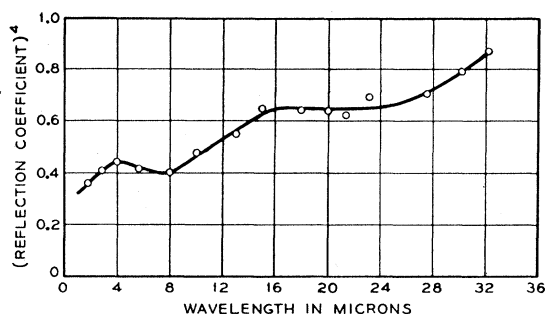


FIG. 2. The fourth power of the reflection coefficient of a single crystal of graphite.

same notation. We confine our attention to the case of linearly polarized light propagated along the  $C$  axis and neglect relaxation processes. This is a good first approximation for the high-temperature experiments which extend only to 12 microns and certainly true for the low-temperature experiments out to 30 microns.

The dielectric constant  $\epsilon(\omega)$  and the conductivity  $\sigma(\omega)$  are given by the expressions<sup>4</sup>

$$\epsilon - 1 = \sum_{\gamma\gamma'\mathbf{k}} \frac{4\pi e^2}{m} \left( \frac{f_{\gamma\gamma'}(\mathbf{k})}{\omega_{\gamma\gamma'}^2(\mathbf{k}) - \omega^2} \right), \quad (1)$$

$$\sigma = \sum_{\gamma\gamma'\mathbf{k}} \frac{\pi e^2}{2m} f_{\gamma\gamma'}(\mathbf{k}) \delta[\omega_{\gamma\gamma'}(\mathbf{k}) - \omega], \quad (2)$$

where  $f_{\gamma\gamma'}(\mathbf{k})$  is the oscillator strength for the transition of one electron from the state with momentum  $\mathbf{k}$  in band  $\gamma$  to the state with momentum  $\mathbf{k}$  in band  $\gamma'$ .  $\omega_{\gamma\gamma'}(\mathbf{k})$  is equal to  $[E_{\gamma'}(\mathbf{k}) - E_{\gamma}(\mathbf{k})]/\hbar$ . If  $\boldsymbol{\eta}$  is a unit vector along the photon polarization and  $\mathbf{p}$  the momentum operator, the oscillator strength is given by

$$f_{\gamma\gamma'}(\mathbf{k}) = \frac{2}{\hbar m} \frac{|\langle \psi_{\gamma}(\mathbf{k}) | \boldsymbol{\eta} \cdot \mathbf{p} | \psi_{\gamma'}(\mathbf{k}) \rangle|^2}{\omega_{\gamma\gamma'}(\mathbf{k})}. \quad (3)$$

According to our present knowledge of the band structure, the Fermi level lies at the corners of the hexagonal Brillouin zone, in a region where there are four  $\pi$  bands with a separation of less than 1 electron volt. The transitions between any two of these bands will involve very small values of  $\omega_{\gamma\gamma'}(\mathbf{k})$  and therefore will give the predominant contributions in the infrared. We therefore make the approximation that the summation over  $\gamma\gamma'$  occurring in (1) and (2) can be restricted to these four bands. In our opinion this is valid because of the overwhelming contribution to  $\epsilon$  from these bands. The calculation will yield a value of the order of 50 for  $\epsilon$ .

We now proceed to evaluate  $f_{\gamma\gamma'}(\mathbf{k})$  and  $\omega_{\gamma\gamma'}(\mathbf{k})$  using the band structure and wave functions given in reference 2. In order to simplify the calculation, we

<sup>4</sup> A. H. Wilson, *The Theory of Metals* (Cambridge University press, Cambridge, 1936), first edition, pp. 127 to 132.

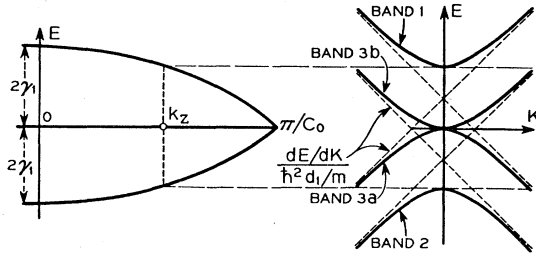


FIG. 3. The four  $\pi$  bands of graphite near a corner of the zone. The figure on the left shows the splitting of the bands in the direction of the hexagonal axis. The figure on the right shows the energy dependence in the hexagonal plane.

neglect the band overlap near the Fermi level and therefore set  $\gamma_2 = \Delta = 0$ . We also neglect the warping of the bands, and therefore choose  $\gamma_3 = 0$ .

As a consequence of these approximations we have the band structure as shown in Fig. 3. There are now only two band parameters left:  $\gamma_1$ , which determines the maximum splitting of the  $\pi$  bands along  $k_z$ , and  $d_1$ , which determines  $dE/dk$  in the  $k_x, k_y$  plane. By setting the band overlap equal to zero, we have assumed a band structure with no free carriers, and we will have to return to this consideration later when we discuss plasma effects. We expect all of the above approximations to be valid, however, when we are dealing with the near infrared where  $\hbar\omega > \gamma_2$  or  $\Delta$ .

The calculation of  $f_{\gamma\gamma'}(\mathbf{k})$  and  $\omega_{\gamma\gamma'}(\mathbf{k})$  is straightforward and yields the following result. The only transitions giving nonzero oscillator strength are between band 3a and band 1 or between 2 and 3b (Fig. 3). Each type of transition gives rise to the same oscillator strength,  $f(\mathbf{k})$ , and frequency difference  $\omega(\mathbf{k})$ .

We express  $\mathbf{k}$  in cylindrical coordinates  $(k_z, K, \alpha)$ , and as in reference 2 define  $\varphi = k_z C_0/2$ , where  $C_0$  is the height of the unit cell, and a quantity  $\Gamma$  by

$$\Gamma^{-2} = 1 + \hbar^4 d_1^2 K^2 / m^2 \gamma_1^2 \cos^2 \varphi. \quad (4)$$

In terms of these parameters, we have

$$f(\mathbf{k}) = d_1^2 \hbar^2 \Gamma (\sin^2 \alpha + \Gamma^2 \cos^2 \alpha) / m \gamma_1 \cos \varphi, \quad (5)$$

$$\omega(\mathbf{k}) = 2\gamma_1 \cos \varphi / \Gamma. \quad (6)$$

From this expression we may evaluate  $\sum_{\mathbf{k}\gamma\gamma'} f(\mathbf{k})$  which enters both  $\epsilon$  and  $\sigma$ . We find<sup>5</sup>

$$\sum_{\mathbf{k}\gamma\gamma'} f(\mathbf{k}) = \frac{4\gamma_1 m}{\pi^2 \hbar^2 C_0} \int_0^{\pi/2} d\phi \int_0^1 \cos \varphi \frac{(1 + \Gamma^2)}{\Gamma^2} d\Gamma. \quad (7)$$

Using (1), (2), (5), (6), (7), and defining a reduced frequency  $x = \hbar\omega/2\gamma_1$ , we obtain

$$\epsilon - 1 = \pi e^2 g_1(x) / \gamma_1 C_0, \quad (8)$$

$$4\pi\sigma/\omega = \pi e^2 g_2(x) / \gamma_1 C_0, \quad (9)$$

<sup>5</sup> The divergence for  $\Gamma=0$  (i.e., large  $K$ ) comes from the fact that for large  $K$ , the bands are no longer hyperboloids. This does not affect the calculation of  $\epsilon$  and  $\sigma$ , which do not depend on such high-energy transitions.

where the functions  $g_1(x)$  and  $g_2(x)$  have been computed numerically and are plotted in Fig. 4. The singularities at  $x=1$  arise from the fact that at this point,  $\hbar\omega$  is equal to the maximum splitting  $2\gamma_1$  between bands 3 and bands 1 and 2. For  $x < 1$  the range of  $k_z$  for which one may have  $\omega(k) = \omega$  steadily decreases, leading to a decrease in  $\sigma$ .

By setting the overlap term  $\gamma_2 = 0$  we have completely neglected the contribution of the free carriers to the optical properties. If we still keep the relaxation time infinite, the intraband transitions of the free carriers will contribute only to  $\epsilon$  and not to  $\sigma$ . The magnitude of this contribution may be evaluated by using the simple model described in reference 2. We set  $\Delta = 0$  as before and replace the hyperbolic bands near  $E_3$  by parabolic bands with a mass proportional to  $\cos \varphi$ . The intraband oscillator strength is then  $m/m^*$ , where  $m^*$  is the effective mass, and the corrected expression for the dielectric constant is

$$\epsilon - 1 = \frac{\pi e^2}{\gamma_1 C_0} \left[ g(x) - 0.43 \frac{\gamma_2}{\gamma_1} \frac{1}{x^2} \right]. \quad (10)$$

The effect of the intraband transitions is to reduce  $\epsilon$  as the reduced frequency  $x$  goes to zero. At a certain frequency  $\omega_\epsilon$ ,  $\epsilon$  goes through zero. Negative values of  $\epsilon$  do not admit any real propagation of an electromagnetic wave and within our approximations the reflection coefficient approaches unity.

The frequency  $\omega_\epsilon$  at which this increase in the reflection coefficient occurs is readily obtained from (10) in terms of  $\gamma_2$  and  $\gamma_1$ . The reflection coefficient will not have a sharp discontinuity as  $\epsilon$  passes through zero,

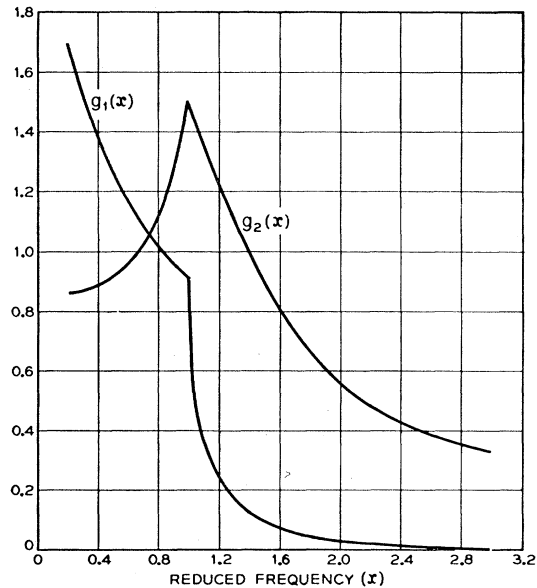


FIG. 4. Numerical values of the functions  $g_1(x)$  and  $g_2(x)$ , which enter Eqs. (8) and (9), shown as a function of the reduced frequency.

since in this region the real part of the conductivity arising from interband transitions is still present.

### DISCUSSION

We are now prepared to compare the calculated and observed reflection coefficients. We shall find that  $\pi e^2 \gamma_1 C_0$  is of the order 50; it is therefore possible to neglect 1 compared to  $\epsilon$ , and the complex dielectric constant  $\bar{\epsilon}$  is given by

$$\bar{\epsilon} = \epsilon - 4\pi i\sigma/\omega = \pi e^2 [g_1(x) - ig_2(x)] / \gamma_1 C_0. \quad (11)$$

For such a large value of  $\bar{\epsilon}$  the reflection coefficient,  $R$ , for a surface normal to the  $C$  axis is given by

$$1 - R = 4 \operatorname{Re} \frac{1}{\sqrt{\bar{\epsilon}}} = \left( \frac{16\gamma_1 C_0}{\pi e^2} \right)^{\frac{1}{2}} \operatorname{Re} \left\{ \frac{1}{[g_1(x) - ig_2(x)]^{\frac{1}{2}}} \right\}. \quad (12)$$

The quantity  $\operatorname{Re}\{1/[g_1(x) - ig_2(x)]^{\frac{1}{2}}\}$  is plotted in Fig. 5 versus  $1/x$ , i.e., versus the wavelength of the radiation measured in units of  $\pi\hbar C_0/\gamma_1$ .

The quantity  $1 - R$  represents the amount of incident energy absorbed in a reflection. According to Kirchoff's law, this is directly proportional to the emissivity  $e_\lambda$ . Comparing Fig. 5 with the experimentally observed curve in Fig. 1 we identify the singularity at  $x=1$  with the region around 4.5 microns. This leads to a value for  $\gamma_1$  of 0.14 eV.

If we fit the center of the curve to the theory, both ends lead to some trouble. At short wavelengths the experimental value of  $e_\lambda$  increases more sharply than theory would predict.

It is just in this region that experimental errors are largest, partly because of the small amount of energy available but more because of the steepness of the black-body curve which places great emphasis on both the temperature measurements and wavelength calibration. In the light of this fact, we are inclined to attribute any discrepancy in this region to experimental error.

At longer wavelengths the experimental value of  $e_\lambda$  drops slowly below the theoretical curve. This may be due to the fact that at such frequencies the collisions of the electrons begin to play an appreciable role (especially at the high temperatures where the emissivity experiments were performed), and this has been completely neglected in our theoretical treatment. This may also be due to the contribution of the intraband transitions to  $\epsilon$ .

The reflectivity experiments performed at low temperatures should, in principle, give more information on the long-wavelength behavior of  $R$  than the emissivity measurements, made at high temperatures.

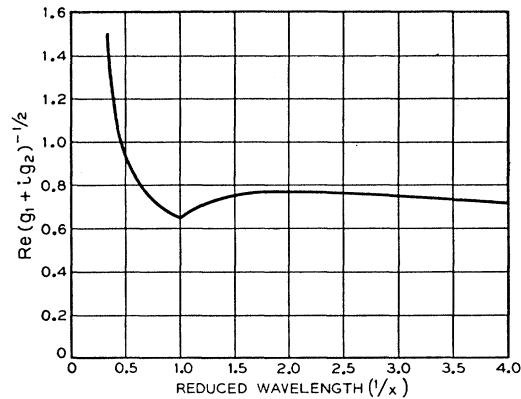


Fig. 5. The real part of  $[g_1(x) + ig_2(x)]^{-1/2}$ , which determines the wavelength dependence of the reflection coefficient, shown as a function of the reduced wavelength  $1/x$ .

Around 4°K, one does not have to worry about electron collisions. On the other hand, they are much harder to interpret, since the light does not have a normal incidence on the crystal. The above calculation cannot therefore apply quantitatively to that case. In practice, one may give a qualitative interpretation of the data which fits with our picture of the energy bands.

We first observe a drop of  $R^4$  between 4 and 8 microns which agrees fairly well with the increase of  $1 - R$  arising between 4 and 7 microns. The place at which the curves bend over is not very well determined, and we feel that in this range, the discrepancies between Figs. 1 and 2 are well within experimental area. Above 8 microns,  $R^4$  increases steadily, which is consistent with the observed behavior of  $1 - R$ . This may be due to the effect of intraband transitions which tend to decrease  $\epsilon$ . Between 16 and 28 microns the curve shows a dip which may be due to the passage through the plasma frequency. This interpretation is substantiated by the value  $\gamma_2 = 0.016$  eV, given by McClure,<sup>1</sup> which yields a plasma frequency  $\omega_\epsilon$  lying around 25 microns.

This evidence of a plasma effect is by no means convincing. Apart from the difficulties arising from an oblique incidence, it may happen that in this range of frequencies the approximation  $\Delta = 0$  is no longer good. Near the crossover of bands 1 and 3, the effective mass approximation is very poor and a complete calculation would be needed in order to interpret properly these results. Such an improvement has not been attempted.

Our results may be summarized as follows: in the short-wavelength limit (from 2 to 8 microns), both emissivity and reflectivity data agree fairly well with the theoretical predictions. They yield a value of the parameter  $\gamma_1$  of about 0.14 eV, which seems a reliable result. There is some evidence of a plasma resonance around 25 microns, which is consistent with our present picture of the graphite energy bands; this last piece of information is not very reliable.